Ultrafast high-resolution magic-angle-spinning NMR spectroscopy

Marion André, Martial Piotto, Stefano Caldarelli, Jean-Nicolas Dumez

Analyst

COMMUNICATION

Ultrafast high-resolution magic-angle-spinning NMR spectroscopy†

Cite this: *Analyst*, 2015, **140**, 3942

Received 3rd April 2015,
Accepted 30th April 2015

DOI: 10.1039/c5an00653h

www.rsc.org/analyst

Marion André,[a] Martial Piotto,[b,c] Stefano Caldarelli[a,d] and Jean-Nicolas Dumez*[a]

We demonstrate the acquisition of ultrafast 2D NMR spectra of semi-solid samples, with a high-resolution magic-angle-spinning setup. Using a recent double-quantum NMR pulse sequence in optimised synchronisation conditions, high-quality 2D spectra can be recorded for a sample under magic-angle spinning. An illustration is given with a semi-solid sample of banana pulp.

The analysis of complex mixtures is a major challenge for the chemist. Nuclear magnetic resonance spectroscopy (NMR) is a powerful tool in this endeavour, which provides extensive information for a large variety of systems with little or no sample preparation. This is particularly true for high-resolution magic-angle-spinning (HR-MAS) NMR spectroscopy, which yields spectra straight from raw material such as biopsies, plant tissues or foodstuffs, inaccessible to other analytical techniques.[1] In many cases, one-dimensional ^{1}H NMR is insufficient to disentangle the complexity of mixtures obtained with no purification. Multidimensional experiments are then essential for identification and quantification, as illustrated in applications such as metabolomics or natural product research.[2] Conventional acquisition strategies, however, require long experimental times that are not compatible with high-throughput studies or the analysis of fragile samples.

Ultrafast NMR provides a significant acceleration of multidimensional NMR, by relying on a spatial rather than temporal dimension to encode NMR interactions.[3] Ultrafast NMR has proven useful to capture transient signals, *e.g.*, in the real-time monitoring of chemical reactions[4] or in combination with hyperpolarization.[5] Spatial encoding has also been exploited for applications of quantitative 2D NMR.[6] The principles of spatial encoding, however, generally assume that sequences of radio-frequency pulses and magnetic field gradients are applied to a static sample. A pioneering study by Frydman and co-workers has shown that solid-state ultrafast magic-angle-spinning NMR spectra can be recorded using a solid-state NMR probe in a microimaging gradient system.[7] The same study, however, noted that no satisfactory spectra could be obtained with the corresponding HR-MAS setup.

In this communication, we show that high-quality ultrafast 2D NMR spectra can be recorded under magic-angle spinning conditions, using a standard HR-MAS setup. Using a recent double-quantum NMR sequence[8] with tailored acquisition and processing steps, we obtain 2D spectra in a single scan for a model solution under magic-angle spinning. We then illustrate the applicability of UF HR-MAS to semi-solid samples with the example of fresh fruit.

Ultrafast NMR relies on a spatial encoding of the NMR interactions. The encoding is achieved with the scheme shown in Fig. 1a. Using a pair of swept radio-frequency pulses played together with magnetic field gradients, spin packets precess under the effect of the chemical shift Ω_i during a time that is proportional to their position z along the encoding axis and acquire a phase:

$$\phi = 4T_e\Omega_i\frac{z}{L},$$

where L is the length of the encoded region, T_e the duration of the encoding pulse. Translating solution-state NMR methods to HR-MAS is not necessarily straightforward, as the possible interference of sample spinning needs to be taken into account.[9] In solution-state NMR, spatial encoding relies on a gradient that is oriented along the cylindrical symmetry axis of the tube. In HR-MAS NMR, an analogous encoding would require perfect alignment of the gradient axis and of the rotation axis (the long axis of the rotor), as well as perfect gradient linearity. In practice, non-idealities result in a modulation of the gradient experienced by the spins during sample

[a]*Institut de Chimie des Substances Naturelles, CNRS UPR 2301, Avenue de la Terrasse, 91190 Gif-sur-Yvette, France. E-mail: jeannicolas.dumez@cnrs.fr*
[b]*Bruker Biospin, Laboratoire d'applications RMN, 34 rue de l'industrie, 67166 Wissembourg, France*
[c]*Strasbourg University, IMIS/ICube Laboratory, 67000 Strasbourg, France*
[d]*Aix Marseille Université, Centrale Marseille, CNRS, iSm2 UMR 7313, 13397 Marseille, France*

†Electronic supplementary information (ESI) available: (i) Materials and methods; (ii) example of spinning sidebands; (iii) conventional HR-MAS spectra of solution of sucrose, fructose and glucose; (iv) conventional HR-MAS spectra of fresh banana. See DOI: 10.1039/c5an00653h

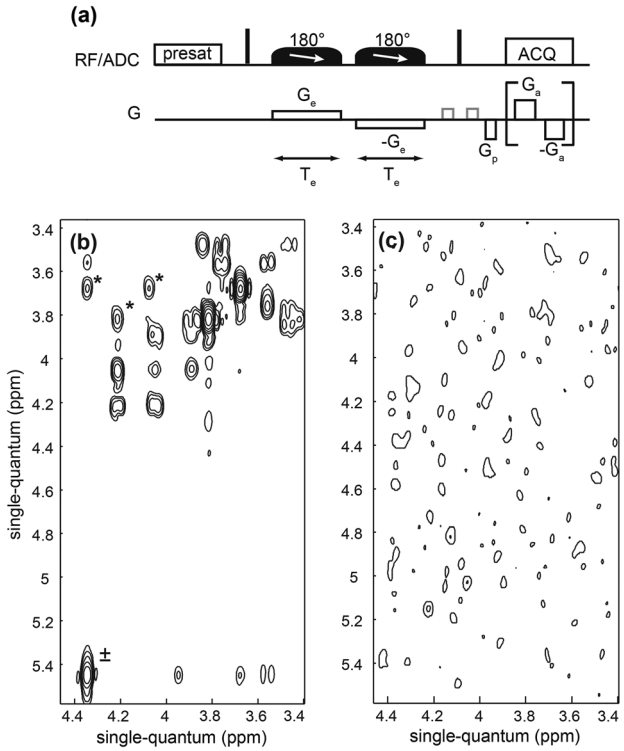

Fig. 1 (a) Pulse sequence for ultrafast COSY. (b and c) Ultrafast HR-MAS COSY spectra of a 500 mM solution of sucrose in D_2O (prepared with 250 μmol of sucrose in 500 μL of D_2O). The period of the detection gradient is $2T_a$ = 1562 μs. In (b), the sample is spinning at a frequency ν_r = 3.84 kHz, which corresponds to a rotor period of T_r = 260 μs and a good quality spectrum is obtained. In (c), the sample is spinning at a frequency ν_r = 4.48 kHz, which corresponds to a rotor period of T_r = 223 μs, resulting in destructive interference Spinning sidebands are marked with an asterisk.

rotation. The most dramatic influence of this modulation is observed at the detection stage, which relies on a periodic, square-wave gradient waveform, analogous to those used in echo-planar spectroscopic imaging. Fig. 1 shows ultrafast NMR spectra of a solution of sucrose obtained with an HR-MAS setup. When the detection period, $2T_a$, is an even multiple of the rotor period, T_r, no destructive interferences are expected, provided that gradient non-idealities remain small. With the HR-MAS setup used here, a typical ultrafast COSY spectrum can be obtained, as shown in Fig. 1b, with a spectrum quality that is comparable to results obtained with a solution-state system. This spectrum was recorded with a single scan in less than 3 seconds, which is orders of magnitude shorter than the time needed for a conventional experiment. In contrast, destructive interference occurs when the detection period is an odd multiple of the rotor period as shown in Fig. 1c. This type of interference was explained through theory and simulations in ref. 7, which also reports that no satisfactory spectra were obtained for a spinning sample with an HR-MAS setup. The interference can be understood by assuming, for example, that the magnetic-field gradient is linear but forms an angle α with the rotor axis, resulting in an additional phase during detection:[7]

$$\phi = \gamma \int_0^t G_0(t')(z\ \cos\ \alpha + r\ \sin\ \alpha\ \cos(2\pi\nu_r t'))\mathrm{d}t'$$

where G_0 is the gradient waveform, ν_r is the spinning rate and r is the distance to the rotor axis. For arbitrary values of the detection period, spinning sidebands are expected and observed at $\pm\nu_r$ of the main peak, as illustrated in the ESI.†

A remaining limitation of the spectrum shown in Fig. 1b is the presence of replicas of some of the peaks, indicated by an asterisk. These replicas may result from additional modulations of the gradient during sample spinning, not accounted for by the current model.

A possible approach to improve the quality of ultrafast homonuclear correlation spectra consists in encoding double rather than single-quantum frequencies[10] in the ultrafast dimension.[8] With the HR-MAS setup, this alternative is especially useful, as it makes it possible to remove not only the large, uninformative auto-correlation peaks, but also the associated images. Ultrafast DQS spectra can be obtained using the pulse sequence described in Fig. 2a. Fig. 2b shows a double-quantum spectrum obtained for the same solution of sucrose, in a single scan and less than 3 seconds. In this case, no spinning sideband is detectable. For comparison, a conventionally acquired DQS spectrum of the same sample is shown in Fig. 2c, using reduced encoding times to mimic the resolution of the ultrafast spectrum. The comparison between Fig. 2b and c shows that the same correlations are observed in both spectra. The relative intensity of the correlation, however, as well as their lineshape, are different. This is a known feature of ultrafast NMR, which is not specific to the HR-MAS case,[11] and which is compatible with quantitative applications of 2D NMR.[6] The conventional spectrum with full resolution is shown in the ESI;† the largest difference in resolution is found in the direct dimension, as in the ultrafast case detection typically lasts of the order of 100 ms because of gradient limitations.

The significant speedup obtained with ultrafast NMR comes at a cost. In particular, the spectral width that can be covered in a single scan is limited by the maximum gradient intensity available. In the case of the HR-MAS probe used here, the nominal maximum gradient intensity is of about 54 G cm^{-1}; with the parameters chosen for the spectrum shown in Fig. 2b, the resulting spectral widths are 1.07 ppm and 2.12 ppm in the conventional and ultrafast dimension, respectively. As a result, the entire set of ^1H resonances for sucrose does not fit in the conventional dimension and a correlation peak is folded, as indicated by the ± symbol. Efficient strategies are available to analyse NMR spectra with peaks that are folded in a Fourier-encoded dimension.[12] Peak folding is also possible in the ultrafast dimension, with several gradient-based strategies.[13] An alternative consists of increasing the spectral width in the conventional dimension by recording several "interleaved" scans.[14] Using this approach together

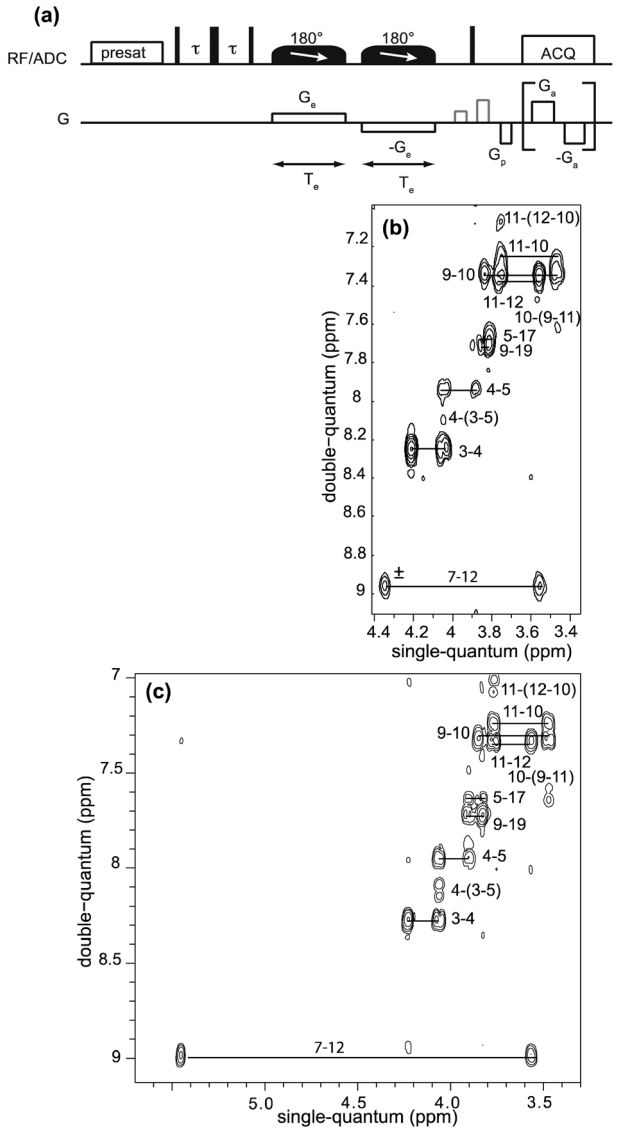

Fig. 2 (a) Pulse sequence for ultrafast DQS. (b) Ultrafast and (c) conventional HR-MAS DQS spectra of a 500 mM solution of sucrose in D_2O. The sample is spinning at a frequency ν_r = 3.84 kHz for the ultrafast experiment. In (b), a single scan is acquired with a spectral width in the conventional dimension of sw_{conv} = 640 Hz and some correlation peaks are folded (indicated by ±).

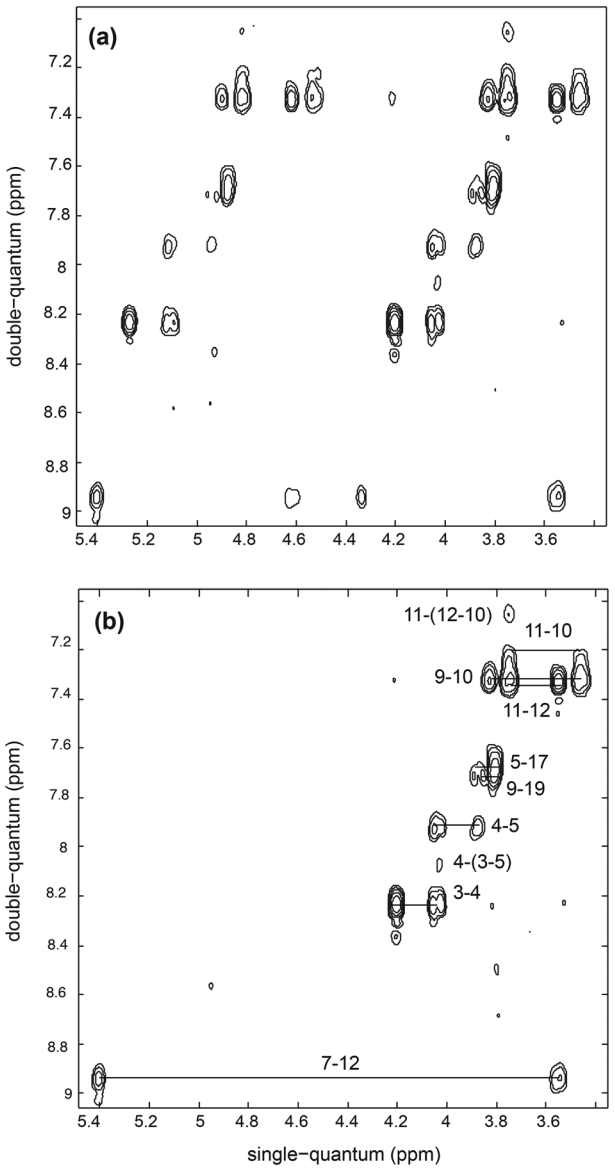

Fig. 3 Ultrafast HR-MAS DQS spectra of a 500 mM solution of sucrose in D_2O obtained with two interleaved scans to increase the spectral width to sw_{conv} = 1280 Hz The sample is spinning at a frequency ν_r = 3.84 kHz. In (a), conventional processing is applied. In (b), a constant phase correction is applied to suppress "ghost" correlation peaks.

with the usual processing strategy for ultrafast NMR spectra, the spectrum shown in Fig. 3a is obtained. With this setup, significant phase instability between successive scans leads to strong "ghost" peaks. Post-processing strategies are available to subtract such ghost peaks.[14b] In this case, however, changing the relative phase of the two interleaves by a constant at the processing stage is sufficient to remove the ghost peaks. The resulting interleaved DQS spectrum of sucrose is shown in Fig. 3b and illustrates how high-quality, spatially encoded spectra can be obtained under magic-angle-spinning conditions on a commercial HR-MAS system.

It should be noted that unsuccessful attempts were made to apply a similar processing strategy to interleaved UF COSY spectra. In this case, neither constant nor linear phase correction yielded spectra free of ghost peaks. Although more advanced phase corrections may in principle be attempted, this further illustrates how the double-quantum NMR is beneficial for spatially encoded experiments.

The analysis reported here relies on the assumption that no macroscopic motion occurs within the rotor during the HR-MAS experiments. Depending on the stability of sample spinning, some internal redistribution may occur within and between the virtual slices of the UFNMR experiments. Such motion would result in a loss in signal intensity, similar to the effect of translational diffusion.[15] In some regimes, the sample

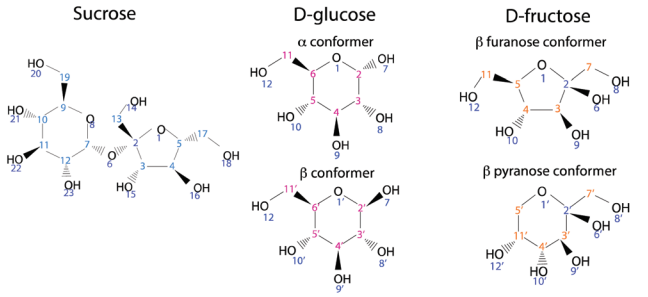

Scheme 1 Chemical structure of sucrose, D-glucose and D-fructose.

density may also be non-uniform along the rotor axis and this would result in changes of the peak lineshape. The analysis of these properties is in progress in our laboratory.

The goal of HR-MAS NMR spectroscopy is to obtain solution-state like spectra of the small mobile components of heterogeneous, semi-solid samples. Foodstuffs are an active area of application of HR-MAS and were chosen here as a model sample;[16] static NMR spectra of foodstuffs are significantly broadened by magnetic susceptibility effects.[16] Specifically, we analysed a sample of fresh banana pulp. Fruit pulp has a complex internal structure, including the solid-like components of cells (lipid membrane, cell wall, membrane proteins...), which are not observed in HR-MAS NMR, and mobile small molecules, which are the target of HR-MAS analyses. The most abundant small molecules in banana pulp are sucrose, glucose and fructose, the structures of which are given in Scheme 1. Other small molecules and in particular amino acids and organic acids are present at lower concentrations. Fig. 4 shows the ultrafast DQS spectrum of a sample of fresh banana, obtained with an HR-MAS setup in less than 90 s. Correlation peaks can be identified for the three most abundant sugars, even in crowded regions of the one-dimensional spectrum. For this example, 4 scans were recorded and averaged to increase the signal-to-noise ratio and identify lower-intensity correlation peaks. While the spectrum shown here for semi-solid sample is not "single-scan", it was still acquired in a much shorter time than a conventional spectra.

Mobile molecules at lower concentrations may be observed with signal averaging or signal enhancement. Interestingly, signal-averaged ultrafast NMR spectra have been shown to be more suitable for quantitative applications than their conventional counterparts.[17] Ultrafast HR-MAS NMR spectroscopy may thus be a useful tool for quantitative studies of raw samples, such as quantitative metabolomics. It is also in principle compatible with other approaches to speed up NMR experiments, such as relaxation enhancement,[18] and applicable to viscous liquids, for which applications of ultrafast NMR in static conditions have been reported.[19]

We have demonstrated the acquisition of ultrafast 2D NMR spectra with a conventional HR-MAS setup and illustrated the fast acquisition of double-quantum spectra for semi-solid samples. UF HR-MAS NMR will be useful for applications of

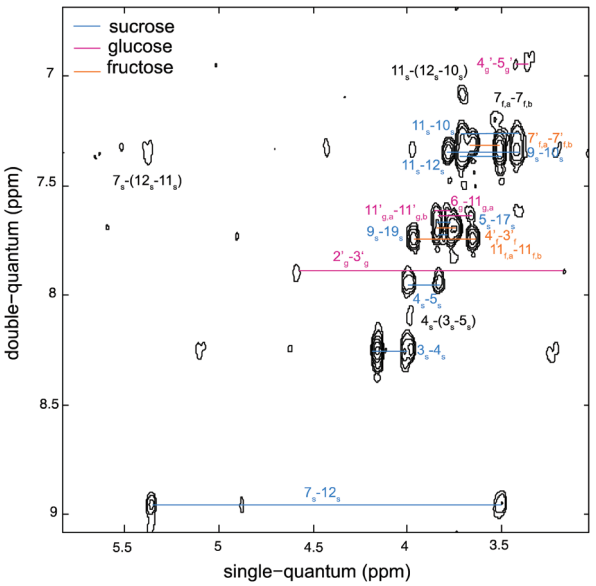

Fig. 4 Ultrafast HR-MAS DQS spectrum of a 10 mg sample of fresh banana. The sample is spinning at a frequency ν_r = 4.53 kHz. Pairs of correlation peaks for the three most abundant sugars in the sample (glucose, fructose and sucrose) are indicated by coloured lines.

NMR that require the fast identification or quantification of small molecules, such as the real-time monitoring of chemical transformations or targeted metabolomics.

We thank Adrien Le Guennec and Patrick Giraudeau for stimulating discussions. We thank the EBSI group from the University of Nantes for providing tools for the acquisition and processing of NMR spectra.

Notes and references

1 (*a*) H. Farooq, D. Courtier-Murias, R. Soong, W. Bermel, W. M. Kingery and A. J. Simpson, *Curr. Org. Chem.*, 2013, **17**, 3013; (*b*) J. C. Lindon, O. P. Beckonert, E. Holmes and J. K. Nicholson, *Prog. Nucl. Magn. Reson. Spectrosc.*, 2009, **55**, 79; (*c*) G. Lippens, M. Bourdonneau, C. Dhalluin, R. Warrass, T. Richert, C. Seetharaman, C. Boutillon and M. Piotto, *Curr. Org. Chem.*, 1999, **3**, 147; (*d*) W. P. Power, *Annu. Rep. NMR Spectrosc.*, 2010, **72**, 111.

2 (*a*) S. L. Robinette, R. Brueschweiler, F. C. Schroeder and A. S. Edison, *Acc. Chem. Res.*, 2012, **45**, 288; (*b*) K. Bingol and R. Brueschweiler, *Anal. Chem.*, 2014, **86**, 47.

3 L. Frydman, T. Scherf and A. Lupulescu, *Proc. Natl. Acad. Sci. U. S. A.*, 2002, **99**, 15858.

4 Z. D. Pardo, G. L. Olsen, M. Encarnacion Fernandez-Valle, L. Frydman, R. Martinez-Alvarez and A. Herrera, *J. Am. Chem. Soc.*, 2012, **134**, 2706.

5 P. Giraudeau, Y. Shrot and L. Frydman, *J. Am. Chem. Soc.*, 2009, **131**, 13902.

6 P. Giraudeau and L. Frydman, *Annu. Rev. Anal. Chem.*, 2014, **7**, 129.

7 M. Gal, C. Melian, D. E. Demco, B. Bluemich and L. Frydman, *Chem. Phys. Lett.*, 2008, **459**, 188.

8 A. Le Guennec, P. Giraudeau, S. Caldarelli and J.-N. Dumez, *Chem. Commun.*, 2015, **51**, 354.

9 M. Piotto, M. Bourdonneau, J. Furrer, A. Bianco, J. Raya and K. Elbayed, *J. Magn. Reson.*, 2001, **149**, 114.

10 (*a*) A. Wokaun and R. R. Ernst, *Chem. Phys. Lett.*, 1977, **52**, 407; (*b*) C. Dalvit and J. M. Bohlen, *Annu. Rep. NMR Spectrosc.*, 1999, **37**, 203.

11 B. Shapira, A. Lupulescu, Y. Shrot and L. Frydman, *J. Magn. Reson.*, 2004, **166**, 152.

12 B. Vitorge, S. Bieri, M. Humam, P. Christen, K. Hostettmann, O. Munoz, S. Loss and D. Jeannerat, *Chem. Commun.*, 2009, 950.

13 (*a*) P. Pelupessy, L. Duma and G. Bodenhausen, *J. Magn. Reson.*, 2008, **194**, 169; (*b*) P. Giraudeau and S. Akoka, *J. Magn. Reson.*, 2010, **205**, 171.

14 (*a*) L. Frydman, A. Lupulescu and T. Scherf, *J. Am. Chem. Soc.*, 2003, **125**, 9204; (*b*) L. Rouger, B. Charrier, M. Pathan, S. Akoka and P. Giraudeau, *J. Magn. Reson.*, 2014, **238**, 87.

15 P. Giraudeau and S. Akoka, *J. Magn. Reson.*, 2008, **195**, 9.

16 (*a*) M. Vermathen, M. Marzorati, D. Baumgartner, C. Good and P. Vermathen, *J. Agric. Food Chem.*, 2011, **59**, 12784; (*b*) T. Delgado-Goni, S. Campo, J. Martin-Sitjar, M. E. Cabanas, B. San Segundo and C. Arus, *Planta*, 2013, **238**, 397; (*c*) M. Valentini, M. Ritota, C. Cafiero, S. Cozzolino, L. Leita and P. Sequi, *Magn. Reson. Chem.*, 2011, **49**, S121.

17 M. Pathan, S. Akoka, I. Tea, B. Charrier and P. Giraudeau, *Analyst*, 2011, **136**, 3157.

18 J. M. P. Vieville, S. Charbonnier, P. Eberling, J. P. Starck and M. A. Delsuc, *J. Pharm. Biomed. Anal.*, 2014, **89**, 18.

19 H.-H. Cai, H. Chen, Y.-L. Lin, J.-H. Feng, X.-H. Cui and Z. Chen, *Food Anal. Methods*, 2014, 1.